Contents lists available at SciVerse ScienceDirect

CIRP Annals Manufacturing Technology

Journal homepage: www.elsevier.com/locate/cirp

A novel methodology to characterize tool-chip contact in metal cutting using partially restricted contact length tools

Gorka Ortiz-de-Zarate[a], Aitor Madariaga[a] (3), Pedro J. Arrazola[a] (1), Thomas H.C. Childs[b] (1)

[a] *Mondragon Unibertsitatea, Faculty of Engineering, Loramendi 4, Arrasate-Mondragón, 20500, Spain*
[b] *School of Mechanical Engineering, University of Leeds, Leeds LS29JT, UK*

A novel methodology to map the friction and normal stress distribution on the rake face using Partially Restricted Contact Length Tools in orthogonal cutting tests is proposed. The influence of cutting speed, feed and coatings on tool-chip friction when machining AISI 1045 is analysed. The results demonstrate that the new methodology can replace the more difficult to use and less robust split-tool method. They confirm two clearly different contact zones: i) the sticking region, governed by the shear flow stress of the workpiece and ii) the sliding region, where the friction coefficient is higher than 1.

Friction, Machining, Tribology, Temperature

1. Introduction

Understanding tool chip friction in metal cutting is key to comprehending thermomechanical loads and tool wear. Correct identification of this friction, together with material flow stress are the main factors which can determine an accurate prediction of the outputs in metal cutting simulation [1]. To gain knowledge of the complex friction interactions at the tool-chip interface and develop accurate models, it is essential to use reliable experimental methodologies. Different experimental techniques have been used such as special tribometers designed for cutting applications, photo-elasticity measurement and machining tests [2].

The uses of special tribometers based on a pin rubbing against a workpiece are widely reported in literature, and a comprehensive review of setups is reported in [2]. These allow the analysis of sliding velocities and contact pressures as close as possible to the machining conditions [3]. However, this methodology has some drawbacks: i) large quantities of material are needed; ii) the surface is not directly refreshed so oxidation may appear; iii) it is difficult to ensure that similar stress distributions and temperatures to those found in machining are achieved; and iv) a constant average friction coefficient value is obtained.

Force measurements in machining tests, resolved parallel and normal to the rake face, remain the most widely used approach for obtaining the average friction coefficient. Albrecht's model corrects the results by eliminating the edge effect [4]. These tests are easy to carry out and give an insight into the friction between tool and chip. Nevertheless, none consider the variations of the friction and normal stresses along the rake face due to the variation of sliding velocity, contact pressure and temperature [3].

To overcome these problems the split-tool methodology was developed [5–6]. It is based on machining experimental tests in which the tool is divided into sections along the rake face (varying the distance from the cutting edge) and measuring the forces in each section of the tool using two dynamometers. The main advantage of this method is that it extracts the contact pressure and shear stress from each rake face section, and therefore maps the distribution of the friction and normal stresses on the rake face. It has major disadvantages, however: i) the complexity of the manufacturing route of the tools; ii) it is not practical to use with coated tools due to the progressive grinding carried out in the clearance face to modify the distance from the cutting edge; and iii) the weakness of the tool section nearest to the cutting edge limits which work materials can be studied. In view of these drawbacks, few researchers have used this friction characterization methodology.

This paper presents the development of a novel method, with the use of tools named here as Partially Restricted Contact Length Tools (PRCLT). The ability of this method to determine rake face friction and normal contact stress distributions is validated by orthogonal machining of an AISI 1045 carbon steel at cutting speeds from 50 to 200 m/min and feeds of 0.2 and 0.3 mm/rev, with both uncoated and TiN-coated cemented carbide tools. For further validation rake face temperatures are also obtained, and the temperature dependence of measured friction stress plateaus are compared to existing published data [7].

2. Methodology

2.1. Overview

The orthogonal machining setup is introduced in Fig. 1a. The insert has a rectangular groove of depth G_d that stops short of the cutting edge, but extends beyond the contact length l_c between the chip and tool. On the right is a plan view of a real example, showing the groove of width G_w separated from the edge by a land of length d_e. It is centrally positioned within the width of cut a_p.

Machining is carried out using a range of inserts with different land lengths d_e. In particular, machining is by radial plunge cutting of ribs pre-machined from a round bar (Fig. 1b), and cutting and thrust forces are measured. Ploughing forces are determined with un-grooved tools following Albrecht's approach [4]. These ploughing forces are removed from the forces with PRCLT tools before calculating the normal and tangential forces (N_r and F_r) on the rake face. N_r and F_r reduce as d_e reduces. The normal σ_n and friction τ_t contact stresses are found from this. It is assumed (see Section 2.3) that the contact stresses outside the groove are not changed by the groove and are uniform across the contact width. Then, if d_e were zero, N_r and F_r would be reduced from their values with an un-grooved tool by the ratio G_w/a_p. When $d_e > 0$, the normal and tangential forces acting over the area $G_w \cdot d_e$ (N_t and F_t)

are obtained from the excess of the force then acting over the forces when $d_e = 0$. Finally σ_n and τ_t at the distance d_e from the cutting edge are obtained from the rate of change of N_t and F_t with d_e (Eqs. 1), as with the split-tool method [5,6]. Fig. 1b illustrates this, with an example. As a check, integrating σ_n and τ_t over the contact should recover N_r and F_r for the un-grooved tool (important for confirming the peak in σ_n).

$$\sigma_n = \frac{1}{G_w}\frac{\mathrm{d}N_t}{\mathrm{d}d_e} \qquad \tau_t = \frac{1}{G_w}\frac{\mathrm{d}F_t}{\mathrm{d}d_e} \tag{1}$$

2.2. Experimental conditions

Two types of tool inserts were selected for this study: i) uncoated carbide tools (WIDIA-TPUN 160308 TTM P/M), and ii) TiN-coated inserts (Sandvik-TPUN 160308 235 P/M with a TiN coating thickness of 4±0.5 µm). The rake and relief angles of both inserts were of 5° and 6° respectively. The clearance face of all inserts was ground to ensure a constant cutting edge radius of 5±1 µm for uncoated inserts, and 14±1 µm for coated. Grooves were made in the rake faces by precision sinking Electro Discharge Machining.

In all cases the groove width was 1±0.02 mm, i.e. $G_w/a_p = 1/3$. This ratio gives a measurable change in forces as d_e is changed, without affecting the chip morphology. Groove depth was 400±50 µm to avoid contact between the chip and the bottom of the groove, while still ensuring the stiffness of the insert. Inserts were prepared with d_e varying in 0.1 mm steps from 0.1 mm to 1.4 mm, longer than the largest value of l_c. Importantly, the minimum value of d_e used in each case was set depending on the cutting condition, so as to not affect the chip morphology and contact length. The geometry of the insert grooves was verified using an optical amplifier and a focus variation device (Alicona IFG4). A total of 8-12 grooved tool inserts were required to identify the friction distribution in each trial of the nine working conditions tested.

The chosen work material was normalised AISI 1045 (92 HRB with a grain size of ASTM 8). In all cases the rib width was $a_p = 3$ mm. Both coated and uncoated inserts were tested at two cutting speeds ($v_c = 100$ and 200 m/min) and two feeds ($f = 0.2$ and 0.3 mm/rev). One additional working condition was tested for uncoated tools ($v_c = 50$ m/min, $f = 0.2$ mm/rev). Each rib of the bar was machined using a single working condition and PRCLT. Several trials were conducted for each value of d_e and working condition using a fresh PRCLT, so as to determine the uncertainty of the results (roughly 10% in stresses). The tests were carried out in a horizontal CNC lathe and a Kistler 9121 dynamometer was used to measure forces. Low-pass filter with frequency of 300 Hz was applied to the data to remove the acquisition signal noise.

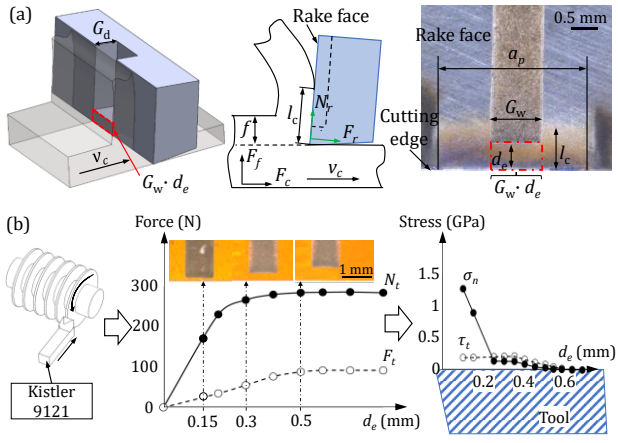

Fig. 1. (a) Basic description of the PRCLT and (b) scheme of the methodology (including example experimental results for TiN-coated insert $v_c = 200$ m/min and $f = 0.2$ mm/rev).

2.3. Confirmation of assumptions

Chips were sectioned to determine thickness both longitudinally and transversely. Contact length was measured by an optical amplifier. The tests were only accepted if no difference between results from PRCLT and un-grooved tools was found. It indicates that contact stresses would be the same for both. Fig.2a is an example of an accepted transverse chip section.

A chemical map analysis of the rake face of the tested inserts using a Scanning Electron Microscope (SEM) confirmed that contact length (represented by the iron deposition) did not vary. It also showed there was no accumulation of iron debris in the bottom of the groove (Fig. 2b) and there was not crater tool wear.

Uniformity of stresses across the width of contact of un-grooved tools was assessed in two ways. Negligible chip thickness changes (t_2 ± 10 µm) are seen at edge of transverse chip sections (Fig. 2a). Further force measurements with un-grooved tools, but varying a_p from 1 to 6 mm, show a strict linear dependence of forces on a_p, with an effectively zero force intercept at zero a_p (Fig. 2c). These support that reducing d_e to zero reduces forces from their values with un-grooved tools by the ratio G_w/a_p.

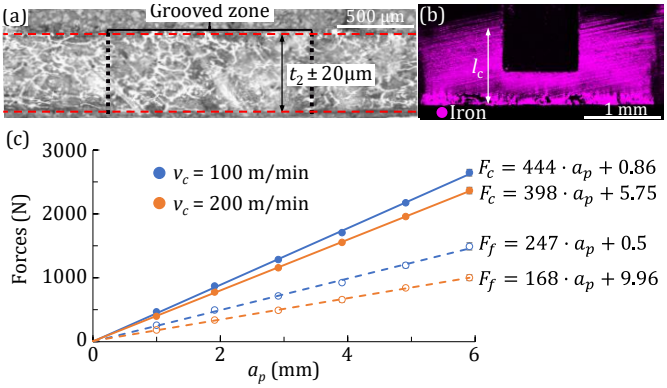

Fig. 2. (a) Transverse cut of the chip ($v_c = 200$ m/min, $f = 0.2$ mm/rev, $d_e = 0.2$ mm and uncoated insert). (b) Iron depositions on the rake face of an uncoated insert ($v_c = 100$ m/min, $f = 0.2$ mm/rev, $d_e = 0.4$ mm). (c) Influence of a_p on forces for $f = 0.2$ mm/rev and two cutting speeds.

2.4. Temperature measurement

Contact temperatures were determined by infra-red observation of specially prepared side faces of tools machining the same AISI 1045 carbon steel, at the same speeds and feeds, as in the main tests but in the form of tubes, as described in previous works [8,9]. It is well known that the maximum temperature on the side face (see Fig. 3a-b) is less than that within the contact [10]. A correction must therefore be made to account for this.

In a previous work [11], based on analysis described by Shaw [12], an approximate value for the maximum temperature rise ΔT_{side} on the tool side face was obtained in terms of the contact length (l_c), width of cut (a_p) and distance (d) from the contact area to the side of the tool (Fig. 3b). Eq. 2 was presented where q is the heat flux into the contact area, and K the tool thermal conductivity.

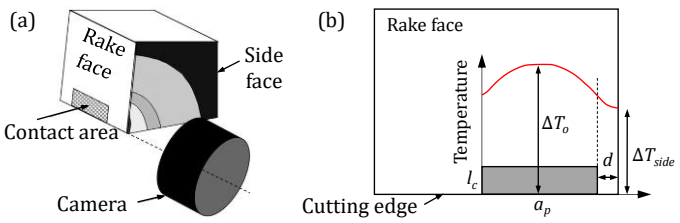

Fig. 3. (a) Schematic view of side face temperature measurement, (b) plan view of the rake face defining the rise of temperature ΔT_o and ΔT_{side}.

In the present study, an additional expression for the temperature rise within the contact, ΔT_o is presented in Eq.3, based on the same analysis. The ratio ΔT_o to ΔT_{side} depends only on l_c, a_p and d. Here the contact temperature rise ΔT_o is obtained from the measured ΔT_{side} by multiplying by that ratio. With fixed d = 0.4 mm, and l_c varying from 0.6 to 1 mm, the ratio ranges from 1.51 to 1.76, in good agreement with observed values [10].

$$\Delta T_{side} = \frac{2ql_c}{\pi K}\left[1 - \frac{d}{l_c}\sinh^{-1}\left(\frac{l_c}{d}\right) + \sinh^{-1}\left(\frac{d+a_p}{l_c}\right) - \sinh^{-1}\left(\frac{d}{l_c}\right)\right] \quad (2)$$

$$\Delta T_O = \frac{2ql_c}{\pi K}\left[0.5\frac{a_p}{l_c}\sinh^{-1}\left(\frac{2l_c}{a_p}\right) + \sinh^{-1}\left(\frac{a_p}{2l_c}\right) + 0.5\ln\left(\frac{3a_p+4d}{a_p+4d}\right)\right] \quad (3)$$

3. Results and discussion

3.1. General behaviour

Fig. 4 sets out the contact stress results. Parts (a-d) show the dependence of normal and friction stress on distance from the cutting edge. These plots confirm two clearly different contact zones, as Zorev's model [13]: i) the sticking region, where the friction stress takes a constant value and ii) the sliding region, where the friction follows the Coulomb's law. Parts (e-f) replot friction stress against normal stress towards the end of the contact, to obtain the local friction coefficients in the Coulomb's law region.

In every respect the uncoated and coated, un-grooved and PRCLT results were as expected, both physically and from the existing literature. It is demonstrated that it is possible to choose a groove dimension that gives a force change large enough to be differentiated reliably (Eqs. 1) for contact stresses to be obtained, without changing the chip formation to make the results not useful (already demonstrated in Section 2.3).

In addition, the experimentally determined apparent friction coefficients μ_{app} (the ratios of rake face total friction to total normal forces) obtained from the uncoated and coated un-grooved tools are presented against $f{\cdot}v_c$ (as a measure of cutting severity) in Fig. 5. As expected, $\mu_{app} < 1$ for all tested conditions. Fig. 5 shows that it decreased with increasing speed or feed, as confirmed by tribometer testing [3]. Moreover, μ_{app} was slightly less for coated than uncoated tools, mainly at more severe conditions, also as reported in literature [14].

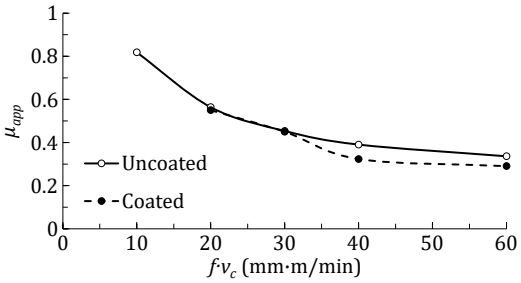

Fig. 5. Apparent friction coefficient from all un-grooved tests.

The contact stress measurements provide two possible reasons for these trends, one from the sticking friction range close to the cutting edge (Fig. 4a-d, d_e/l_c < 0.15-0.25), and the other from the sliding region (Fig. 4a-d, d_e/l_c>0.15-0.25). The following subsections discuss separately the tool-chip interactions within these two regions, supported by contact temperature analysis and results reported by other authors.

3.2. Sticking region

It is well established that the friction stress plateau is found close to the cutting edge and depends on the temperatures reached in this contact region. Fig. 6 shows this paper's rake face tool temperature results: (a) the increase of contact temperature with $f{\cdot}v_c$ and (b) the dependence of the friction stress plateau on the temperature. Both include results from split-tool tests with a zero rake angle tool, f = 0.1, 0.2 mm/rev, and v_c from 50 to 250 m/min, on a normalised AISI 1045 steel, although of unknown grain size [7]. Fig. 6b also includes, as the dashed line, an estimate of expected thermal softening of the steel. It is expressed (right hand axis) as the flow stress at temperature relative to the flow stress at room temperature and comes from work that successfully predicts crater wear of an uncoated tool [15].

The present PRCLT results and these previous ones overlap. While there is indeed a large uncertainty range in Fig. 6b, it does not obscure the thermal softening trend. Thus, in addition to the stress distribution results in Fig. 4, Fig. 6 demonstrates in detail the validity of the PRCLT method.

In addition, the friction stress plateau presents a slightly lower value for the coated than uncoated tools. Hence, the apparent friction coefficient is smaller for the coated than the uncoated

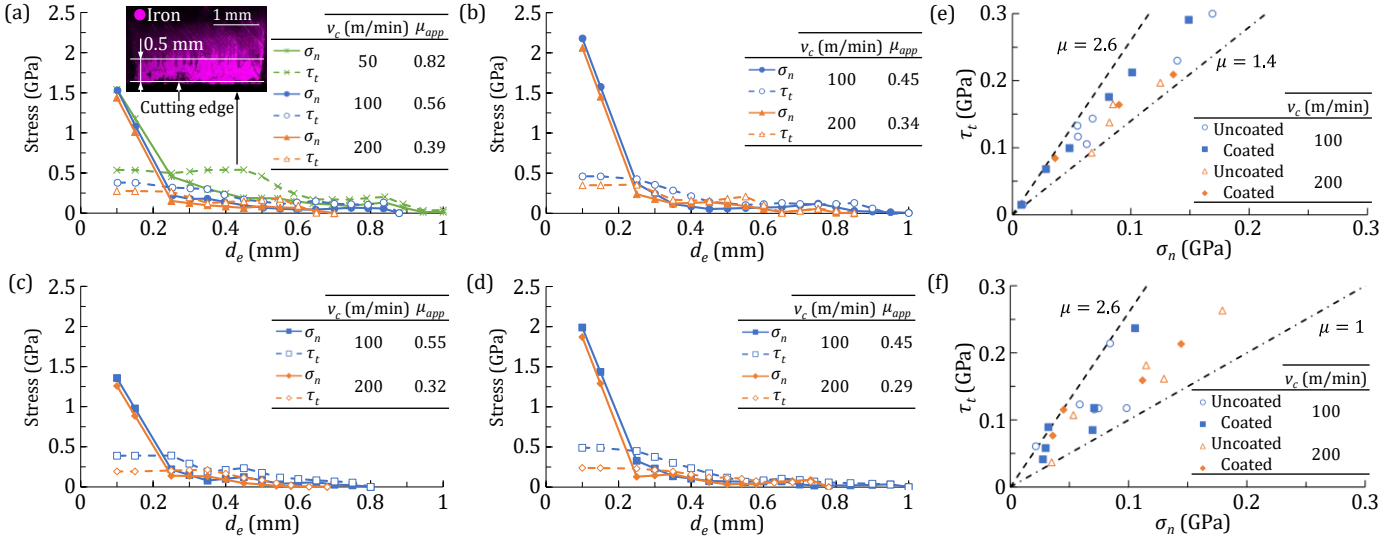

Fig. 4. Normal and friction stress results of (a) uncoated tools for f = 0.2 mm/rev (includes a SEM image of iron transferred on to the rake face for v_c = 50 m/min), (b) uncoated tools for f = 0.3 mm/rev, (c) coated tools for f = 0.2 mm/rev and (d) coated tools for f = 0.3 mm/rev. Local friction coefficient in the sliding region of (e) f = 0.2 mm/rev and (f) f = 0.3 mm/rev.

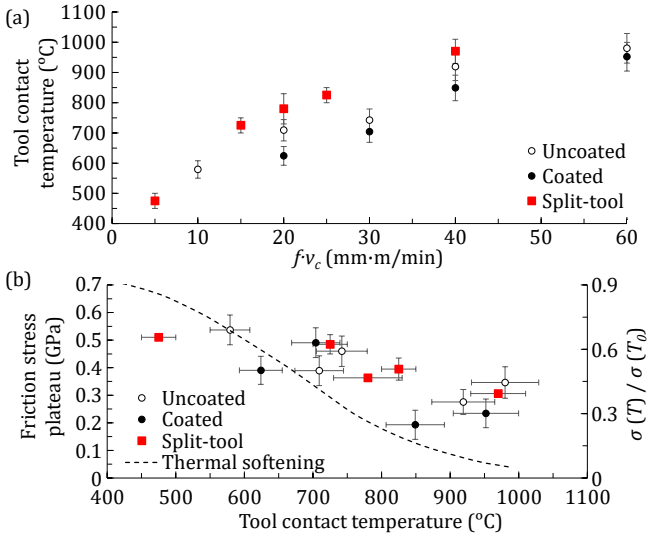

Fig. 6. (a) Tool contact temperature against severity ($f{\cdot}v_c$), (b) relationship between plateau stress and tool contact temperature. Expected relative thermal softening of steel AISI 1045 from [15] is added (with its scale to the right). Both graphs include split-tool results [7].

tools. The probable cause of this lower friction stress is the higher temperature of the chip, due to the tribological effect of the coating [14]. This, in turn, increases the temperature of the chip relative to the tool and leads to a greater thermal softening, mainly at high cutting speeds. Therefore, the main cause of the lower μ_{app} for coated tools might be due to the condition of the friction stress plateau region.

The cutting speed has great influence on the friction stress plateau, while the feed impacts the peak normal stress (see Fig. 4a-d). The increase of the cutting speed reduces the friction stress plateau due to the increase of the contact temperature, causing thermal softening, as previously observed. The increase of the feed from 0.2 to 0.3 mm/rev for any of the conditions, produces an average increase of the peak normal stresses of 630±20 MPa close to the cutting edge, even though the specific forces decrease when increasing the feed.

Interestingly, the PRCLT method reveals a significantly longer friction stress plateau region at the cutting speed of 50 m/min, than at the other speeds. More detailed observations of the insert used in this test confirmed the presence of adhered material on the rake face up to a distance d_e of 0.5±0.1 mm, which roughly matches the plateau length (Fig. 4a). This further validates the method.

3.3. Sliding region

Away from the edge, Fig. 4e-f show a Coulomb's friction coefficient > 1 for both coated and uncoated tools, but with a large scatter (from ≈ 1.0 to 2.6). Large values are known from previous split-tool tests [5-7] and indeed were originally inferred by Zorev [13]. It should be noted that the largest values of the local friction coefficient are found at the end of the contact length, where normal stresses decrease significantly. Therefore, in this final region, small differences in the normal stress can lead to high variations in the determination of the friction coefficient.

The increase of the cutting speed or feed produces slight reductions of the local friction coefficient, similar to that which was observed with the sliding velocity when identifying the apparent friction coefficient through pin-on-disk approach [2].

Fig. 4a-d do show a shorter contact length for the coated than uncoated tools, as also observed in the literature [14,16]. Rech attributes this to a lower adhesion of a TiN coating to steel [14]. Both researches also observed a lower tool temperature for coated rather than uncoated tools, as in the present work (see Fig. 6a).

4. Summary and conclusions

A novel experimental method for mapping normal and shear stress distributions on the rake face is presented. This method is simpler and more robust than the split-tool approach. Stresses are obtained from changes of cutting and feed forces when the rake face of a tool is partially restricted (PRCLT or Partially Restricted Contact Length Tools), using grooves made by precision sinking Electro Discharge Machining.

The implementation of the method, and results from machining an AISI 1045 steel with uncoated carbide tools and for the first time with TiN-coated carbide tools are reported. It is demonstrated that a PRCLT can be designed, from which stress distributions can be determined without significantly changing chip formation from its state in un-grooved tools.

The validation results are in agreement with published data. The results show a sticking region in which friction stress plateau is affected by thermal softening and in which the normal stress peaks sharply at the cutting edge. A sliding region in which the local friction coefficient is > 1 can also be observed.

Using a coating reduces the tool-chip contact length and causes a lower tool temperature produced by the tribological effect of the coating. This causes the chip temperature to increase, contributing to greater thermal softening in the chip, and a reduced friction stress plateau and apparent friction coefficient.

Acknowledgements

The authors hereby thank the INTOOL II (KK-2020/00103) and SURFNANOCUT (RTI2018-095463-B-C21/C22) projects and the grant for Education and Training of Research Staff (PRE_2017_1_0394). In addition, we thank Mr. Denis Soriano and Dr. Mikel Saez-de-Buruaga for their technical support in the temperature measurements and analysis.

References

[1] Arrazola, P.J., Özel, T., Umbrello, D., Davies, M., Jawahir, I.S., 2013, Recent advances in modelling of metal machining processes, Annals of the CIRP, 62/2:695–718.
[2] Melkote, S. N., Grzesik, W., Outeiro, J., Rech, J., Schulze, V., Attia, H., Arrazola, P.J., M'Saoubi, R., Saldana, C., 2017, Advances in material and friction data for modelling of metal machining, Annals of the CIRP, 66/2:731-754.
[3] Rech, J., Arrazola, P.J., Claudin, C., Courbon, C., Pusavec, F., Kopac, J., 2013, Characterisation of friction and heat partition coefficients at the tool-work material interface in cutting, Annals of the CIRP, 62/1:79-82.
[4] Albrecht, P., 1960, New developments in the theory of the metal-cutting process: part I. The ploughing process in metal cutting, ASME J. Manuf. Sci. Eng., 82/4:348-357.
[5] Kato, S., Yamaguchi, K., Yamada, M., 1972, Stress Distribution at the Interface Between Tool and Chip in Machining, ASME J. Manuf. Sci. Eng., 94/2:683-689.
[6] Maekawa, K., Kitagawa, T., Childs, T.H.C., 1997, Friction characteristics at tool-chip interface in steel machining, Tribology Series, 32:559-567.
[7] Childs, T.H.C., 1998, Material property needs in modeling metal machining, Machining science and Technology, 2/2:303-316.
[8] Armendia, M., Garay, A., Villar, A., Davies, M.A., Arrazola, P.J., 2010, High bandwidth temperature measurement in interrupted cutting of difficult to machine materials, Annals of the CIRP, 59/1:97-100.
[9] Saez-de-Buruaga, M., Soler, D., Aristimuño, P.X., Esnaola, J.A., Arrazola, P.J., 2018, Determining tool/chip temperatures from thermography measurements in metal cutting, Applied Thermal Engineering, 145:305-314.
[10] Arrazola, P.J., Aristimuno, P., Soler, D., Childs, T., 2015, Metal cutting experiments and modelling for improved determination of chip/tool contact temperature by infrared thermography, Annals of the CIRP, 64/1:57-60.
[11] Soler, D., Childs, T.H., Arrazola, P.J., 2015, A note on interpreting tool temperature measurements from thermography, Mach. Sci. Technol., 19/1:174-181.
[12] Shaw, M.C., 1984, Metal cutting principles, Clarendon, Oxford. Ch. 12.
[13] Zorev, N.N., 1963, Inter-relationship between shear processes occurring along tool face and shear plane in metal cutting, International research in production engineering, 49:143-152.
[14] Rech, J., 2006, Influence of cutting tool coatings on the tribological phenomena at the tool–chip interface in orthogonal dry turning, Surface and Coatings Technology, 200/16-17:5132-5139.
[15] Saez-de-Buruaga, M., Aristimuño, P., Soler, D., D'Eramo, E., Roth, A., Arrazola, P.J., 2019, Microstructure based flow stress model to predict machinability in ferrite–pearlite steels, Annals of the CIRP, 68/1:49-52.
[16] M'Saoubi, R., Chandrasekaran, H., 2004, Investigation of the effects of tool micro-geometry and coating on tool temperature during orthogonal turning of quenched and tempered steel, Int. J. Mach. Tools Manuf., 44/2-3:213-224.